MAPAN-JOURNAL ,
Publisher: METROLOGY SOC INDIA , NPL PREMISES,
Address: DR K S KRISHNAN MARG, NEW DELHI, INDIA,
ISSN / eISSN:0970-3950 / 0974-9853,
Volume 26-Issue 1-(2026)
DOI:https://doi-001.org/1025/17720167408852

A Computational Thermodynamics Approach to Phase Stability in Fe–Ti Alloys for Sustainable and Durable Infrastructure Steel: DFT–CALPHAD Modeling and Fe–Ti–Ag Extension

Anhar Miloudi [1], Fouzia Adjadj [2], Bentrar Hakim[3], Rachid Rabehi [4], Fidjah Abdelkader[5] , Yacine Djaballah[6], Belgacem bouzida[7], Khaled Boulaiche[8]

[1,2,6,7] Laboratory of Physical and chemical study of materials (LEPCM), University of Batna 1, Physics Department, Faculty of Material Sciences, Algeria.
[3] Center of Research in Mechanics (CRM), BP N73B, Ain El Bey, 25021 Constantine, Algeria.
[4] Faculty of Civil Engineering, University of Science and Technology Houari Boumediene (USTHB), BP 32 El Alia, Bab Ezzouar, 16111 Algiers, Algeria.
[5] Laboratory of Civil engineering and sustainable development, University of Djelfa, Algeria.
[8] Laboratory of Applied Energetics and Materials (LAEM), Faculty of Sciences and Technology, Process Engineering Department, MSBY Jijel University, Algeria.

Submit: 23/02/2025, Accepted: 14/11/2025, Publication: 24/02/2026

Abstract

This work develops a combined computational framework to evaluate phase stability and property trends in Fe–Ti-based alloy systems with relevance to durable infrastructure steels. The study couples density functional theory (DFT) calculations with CALPHAD thermodynamic modeling in order to link fundamental energetics with phase-equilibrium predictions across practical temperature and composition ranges. First-principles calculations are used to determine formation enthalpies and elastic properties of key Fe–Ti intermetallic compounds, providing quantitative descriptors that support both stability assessment and property interpretation. In parallel, the Fe–Ti binary phase diagram is reassessed using the CALPHAD approach, with thermodynamic parameters calibrated against the computed energetic data. The resulting description enables a clearer identification of stability domains associated with FeTi- and Fe_2Ti-related phases and provides a consistent basis for discussing phase evolution under thermal processing conditions that are relevant to steel fabrication routes. Beyond the binary level, the analysis is extended to the Fe–Ti–Ag ternary system to quantify the influence of Ag additions on phase stability trends and to establish baseline information that may be useful for future alloying or surface-engineering strategies targeting combined mechanical performance and functional behavior. Overall, the proposed DFT–CALPHAD workflow offers a coherent route for predicting phase stability in Fe–Ti-based systems and for supporting durability-driven materials design in long-service engineering applications.

Keywords: Infrastructure steel; Fe–Ti alloys; CALPHAD; density functional theory (DFT); phase stability; mechanical properties.

Introduction

Durability has become a central design requirement for modern civil infrastructure. Bridges, marine structures, industrial facilities, pipelines, water and wastewater systems, and exposed steel buildings are expected to operate safely for decades while being subjected to complex mechanical loading, thermal cycling, humidity variations, and chemically aggressive exposure. In many real projects, the governing factor for service life is not the initial strength of the material but the gradual deterioration caused by corrosion, environmental attack, and microstructure-sensitive damage accumulation. Corrosion, in particular, is repeatedly identified as one of the most expensive and disruptive degradation mechanisms, imposing heavy maintenance burdens and reducing the reliability of both steel and reinforced concrete systems. Global assessments have emphasized that corrosion represents a major economic loss, motivating research strategies that aim to extend service life through improved materials and predictive design methodologies [1].

For reinforced concrete (RC) structures, corrosion of embedded steel reinforcement remains one of the most critical durability threats. Chloride ingress in marine environments and de-icing salt exposure, as well as carbonation in urban atmospheres, can depassivate the reinforcement surface and trigger electrochemical corrosion processes. Once corrosion begins, the expansion of corrosion products generates internal stresses that promote cracking and spalling, which in turn accelerates moisture and chloride transport and causes faster deterioration. Recent reviews confirm that chloride-induced corrosion remains a dominant mechanism limiting RC durability and that addressing it requires both improved material design and better predictive understanding of exposure-driven damage evolution [2]. In parallel, a wide body of research has explored protective measures such as coatings, corrosion inhibitors, cathodic protection, and alternative reinforcements, yet long-term infrastructure performance still strongly depends on the intrinsic stability of steel microstructure and phase constitution, especially under variable thermal and chemical histories [3].

In steel structures and steel bridges, atmospheric corrosion is another major concern. Exposed steel components experience wet–dry cycles, fluctuating oxygen availability, deposition of chlorides and sulfates, and microclimatic effects that vary significantly across a structure. Weathering steels are widely used to reduce maintenance costs by developing protective rust layers

under favorable conditions. However, field performance demonstrates that such protection is not guaranteed in all environments, particularly under high chloride loads, poor drainage conditions, or persistent moisture. Several studies and reviews highlight that the protective character of the rust layer depends strongly on alloy chemistry, microstructure, and the long-term stability of corrosion products formed during cycling exposure [4,5]. These observations underline a key point for civil engineering materials: corrosion resistance is not only a function of bulk composition, but also a consequence of phase stability, transformation pathways, and microstructure development during fabrication and service.

The need for durable steel systems has therefore strengthened interest in alloy design strategies that offer robust strength–toughness performance while limiting degradation in harsh environments. Among the different alloying approaches, titanium occupies an important position. Titanium is widely employed as a microalloying element in steels, strongly influencing precipitation behavior, grain refinement, inclusion modification, and strengthening mechanisms. A comprehensive review on titanium microalloying emphasizes that Ti can significantly improve the mechanical performance of low-alloy steels through microstructure control and precipitation hardening, enabling high-performance steels with optimized processing routes [6]. In infrastructure applications, these effects are of high relevance because structural steels are often required to deliver both high strength and reliable fracture resistance, especially in welded zones and in thick sections subjected to complex residual stress fields.

Beyond microalloying, the Fe–Ti system is also characterized by the formation of ordered intermetallic compounds such as FeTi and Fe_2Ti. Intermetallic phases in steels are frequently treated with caution due to their potential brittleness, yet their presence and stability can play a decisive role in mechanical response and in the performance of heat-affected zones during welding or thermal cycling. In practice, civil engineering steels are subjected to manufacturing steps that may locally reach high temperatures, and long-term service may expose components to intermediate temperatures or repeated thermal fluctuations. Under such conditions, phase transformations and intermetallic precipitation may become important, particularly if alloy design pushes compositions near phase boundaries. Therefore, building a reliable thermodynamic description of the Fe–Ti system is not simply a theoretical exercise—it is a practical requirement for predicting microstructural stability and avoiding unexpected embrittlement risks in infrastructure steels.

Phase diagrams are the cornerstone of such predictive design. They provide a map of stable and metastable phases as a function of temperature and composition, offering guidance for alloy selection, processing windows, and heat-treatment strategies. The CALPHAD method (CALculation of PHAse Diagrams) has become a widely adopted quantitative framework for modeling phase equilibria in multi-component systems. Rather than relying purely on experimental mapping, CALPHAD describes phase stability through Gibbs energy functions calibrated against experimental and computational datasets. This methodology enables thermodynamic predictions across broad composition and temperature ranges, even when experimental data are incomplete. As summarized in CALPHAD-focused Springer references, the approach has become the modern standard for thermodynamic assessment and phase diagram development in complex alloy systems [7]. For civil engineering steels, CALPHAD provides a valuable tool for predicting equilibrium phase fractions, identifying potential intermetallic stability zones, and supporting processing decisions relevant to structural integrity.

However, CALPHAD modeling depends on the quality and completeness of its underlying energetic and thermodynamic data. For phases that are difficult to isolate experimentally or that exist only within narrow stability fields, experimental thermodynamic information may be sparse or uncertain. This limitation has motivated the integration of first-principles calculations into thermodynamic assessments. Density functional theory (DFT), often referred to as ab initio computation in materials modeling, offers a high-precision route to calculate formation enthalpies, elastic constants, and electronic structures from fundamental physics. When used in combination with CALPHAD, DFT results can serve as energetic anchors that improve the consistency and predictive capacity of thermodynamic databases. Progress in DFT-informed thermodynamic modeling has been explicitly discussed in the literature, including works demonstrating how first-principles energetics can support CALPHAD development and improve reliability for complex alloy design [8,9]. This integrated strategy is aligned with the broader ICME (Integrated Computational Materials Engineering) vision, which promotes multiscale computational tools to accelerate alloy development and reduce reliance on costly trial-and-error experimentation [10].

From the viewpoint of civil engineering and construction materials, such computational integration is increasingly important. Infrastructure steels and metallic components are expected to balance strength, ductility, weldability, and environmental resistance over long service lifetimes. Yet these properties are governed by microstructure, and microstructure is fundamentally linked to phase stability. Welding, for example, produces complex thermal histories where local heating and

cooling may promote the formation or dissolution of phases that significantly influence hardness, toughness, and susceptibility to cracking. CALPHAD-based thermodynamic modeling has been increasingly applied to joining and welding-related metallurgy, supporting the interpretation of microstructural evolution and phase stability under welding conditions [11]. By providing a quantitative basis for predicting which phases may appear during thermal cycles, such modeling contributes to improved control of mechanical performance and reliability in structural applications.

While durability and corrosion resistance are central to civil engineering, modern infrastructure also increasingly demands multifunctionality. In buildings and public spaces, surface hygiene, contamination control, and resistance to biofouling can become important performance requirements, particularly in transport infrastructure, healthcare-adjacent facilities, and water-contact systems. Silver-containing metallic surfaces and coatings have attracted attention because of silver's well-established antimicrobial activity. Reviews and research studies report that Ag-based surface engineering can significantly reduce microbial adhesion and viability, offering potential functional advantages beyond mechanical performance alone [12-14]. Although silver is not a conventional alloying addition for structural steel in bulk form, it is relevant for surface engineering routes, including coatings, claddings, and near-surface modifications, where localized Ag can deliver functional performance without compromising bulk structural properties. Such concepts may become more relevant as infrastructure materials design evolves toward life-cycle performance and multi-criteria optimization[15].

In this broader framework, investigating the Fe–Ti–Ag ternary system becomes meaningful as a foundational thermodynamic step. The ternary extension is not intended to suggest Ag as a standard bulk element in construction steels, but rather to provide phase-equilibria insight that can support future surface-alloy or hybrid strategies. Ternary thermodynamic descriptions also help quantify whether Ag additions shift stability domains or alter the tendency for intermetallic formation in Fe–Ti-based alloys. Such information is essential if one aims to develop multifunctional metallic layers that combine structural durability with functional properties relevant to the built environment. From a database-development and computational design standpoint, ternary systems are also a natural next step, since realistic steels and surface-engineered alloys are rarely binary [16].

Accordingly, the present work applies a dual theoretical approach to the Fe–Ti system and extends the analysis toward Fe–Ti–Ag. First, ab initio calculations are employed to obtain high-precision energetic data and property descriptors for relevant Fe–Ti intermetallic phases. These calculations provide formation enthalpies and elastic parameters that are important for understanding both phase stability and mechanical response. Second, a CALPHAD-based reassessment of the Fe–Ti binary system is performed to reproduce phase equilibria over a wide range of temperatures and compositions. The thermodynamic modeling is calibrated using the computed energetic data to improve the quantitative reliability of predicted equilibria. Finally, the investigation is expanded to the Fe–Ti–Ag ternary system in order to examine the thermodynamic influence of silver additions on stability trends and to provide baseline information for future alloying or surface-engineering concepts aimed at enhancing performance.

The main objective of this study is to establish a consistent thermodynamic and property-oriented description of Fe–Ti-based alloy systems using a coupled DFT–CALPHAD methodology. Ab initio calculations are employed to provide reliable energetic and mechanical descriptors of the FeTi and Fe_2Ti intermetallic compounds, which are subsequently used to support and calibrate a CALPHAD reassessment of the Fe–Ti binary phase diagram over a wide temperature–composition range. In addition, the work is extended to the Fe–Ti–Ag ternary system to quantify the influence of Ag additions on phase stability trends and to provide baseline thermodynamic information for future durability-driven alloying and surface-engineering concepts. The novelty of this contribution lies in the integrated use of first-principles energetics and CALPHAD modeling to deliver a coherent phase stability framework that connects fundamental thermodynamics with performance-oriented considerations relevant to long-service infrastructure steels.

2. Materials and Methods

2.1. Study workflow and scope

This work relies on a dual computational strategy to describe phase stability and property trends in Fe–Ti-based alloy systems, with an additional extension toward Fe–Ti–Ag. The overall workflow is designed to connect two complementary levels of description. First, density functional theory (DFT) is used to calculate energetic and mechanical descriptors for the main Fe–Ti intermetallic phases of interest (notably FeTi and Fe_2Ti). These results provide a reliable atomistic baseline, particularly for formation enthalpies and elastic behavior. Second, a CALPHAD thermodynamic assessment is performed to build a consistent description of phase equilibria over

broad temperature–composition ranges. The DFT energetic information is then used to support the calibration of thermodynamic parameters and to strengthen the physical consistency of the reassessed phase diagram. This combined approach enables the discussion of stability domains and trends in a quantitative way that is directly useful for interpreting microstructure development under thermal processing conditions.

2.2. First-principles calculations (DFT)

2.2.1. DFT formalism and computational implementation

Electronic-structure calculations were performed within the Kohn–Sham formulation of density functional theory (DFT) [17] using the Vienna Ab initio Simulation Package (VASP) [18]. The interaction between valence electrons and ionic cores was treated using the projector augmented-wave (PAW) method [19], while exchange–correlation effects were described using the generalized gradient approximation in the Perdew–Burke–Ernzerhof (PBE) form [20]. This setup provides a reliable and widely adopted framework for evaluating the energetic stability and structural properties of Fe–Ti intermetallic compounds.

2.2.2. Structural models, relaxation, and numerical settings

Crystal structures of the investigated Fe–Ti intermetallic compounds were constructed based on their reported stable configurations. For each phase, geometry optimization was performed to obtain equilibrium lattice constants and relaxed atomic positions prior to extracting energetic and mechanical properties. A plane-wave kinetic energy cutoff of **500 eV** was adopted in all calculations to ensure stable total-energy convergence and consistent comparison between different phases. Brillouin-zone sampling was performed using Monkhorst–Pack k-point meshes [21], selected to provide converged total energies and stresses for each structure. Structural relaxation was continued until the residual forces on atoms were reduced to sufficiently small values and the total energy variations between successive ionic steps became negligible. These settings were chosen to ensure that computed formation energies and elastic responses reflect equilibrium structures, which is essential when such results are later used as quantitative inputs for thermodynamic modeling.

2.2.3. Formation enthalpy calculations

The energetic stability of the investigated Fe–Ti intermetallic compounds was evaluated using the enthalpy of formation computed from first-principles total energies. For a compound with composition Fe_nTi_m, the formation enthalpy per atom was calculated as:

$$\Delta H_{Fe(n)Ti(m)} = E_{Fe(n)Ti(m)} - \frac{1}{m+n}\left(nE_{Fe(n)} + mE_{Ti(m)} \right) \quad (1)$$

Where $E_{Fe(n)Ti(m)}$ is the DFT total energy of the relaxed intermetallic structure, and $E_{Fe(n)}$ and $E_{Ti(m)}$ are the DFT total energies of elemental iron and titanium in their stable reference states (BCC_A1 for Fe and HCP_A3 for Ti).

This definition provides a consistent basis for comparing stability trends among Fe–Ti compounds and serves as a reliable energetic anchor for the subsequent CALPHAD reassessment, especially in composition ranges where experimental thermochemical data are limited or uncertain.

2.3. Mechanical property evaluation from elastic constants

2.3.1. Elastic stiffness tensor and polycrystalline moduli

Elastic constants were determined from the DFT stress–strain response by applying a set of small, symmetry-consistent deformations to the relaxed structures and calculating the resulting stress tensors. The computed elastic stiffness matrix (C_{ij}) was then used to assess mechanical behavior and to derive polycrystalline mechanical properties. Bulk modulus (B) and shear modulus (G) were obtained using standard averaging procedures. In the present study, the Voigt and Reuss bounds were first evaluated, and the Hill average was then employed as a practical estimate of polycrystalline moduli [22]. This approach is widely used because it provides a stable link between single-crystal stiffness and engineering-relevant mechanical indicators.

2.3.2. Derived mechanical descriptors

From the elastic moduli, Young's modulus (E) and Poisson's ratio (nu) were calculated using standard isotropic relations. In addition, the ratio (B/G) (often used as a qualitative ductility/brittleness indicator) was computed to support comparative discussion between FeTi and Fe_2Ti. While such descriptors do not replace experimental mechanical testing, they provide an informative first-order basis to interpret stiffness and deformation tendencies of intermetallic phases. In the context of structural steels and infrastructure materials, these mechanical trends are relevant because the formation of hard but brittle intermetallic phases may influence damage sensitivity, especially after thermal processing steps such as welding or heat treatment.

2.4. Optical property calculations (supporting analysis)

Optical properties were evaluated as complementary indicators of functional response, particularly to maintain consistency with the original scope of the work. Optical spectra were obtained from the frequency-dependent dielectric function derived from the electronic structure results. From the dielectric response, standard optical quantities were extracted, including reflectivity, absorption coefficient, refractive index, and optical conductivity. While the civil engineering framing of the paper emphasizes durability and long-service performance, these results remain valuable for broader functional interpretation and for documenting the contrast between FeTi and Fe_2Ti in terms of electronic/optical behavior.

2.5. CALPHAD thermodynamic modeling

2.5.1. Thermodynamic background and modeling strategy

Thermodynamic calculations were carried out using the CALPHAD method, which provides a structured and quantitative framework to describe Gibbs free energies of phases and to compute equilibrium phase diagrams across wide composition and temperature ranges [23]. Within CALPHAD, each phase is represented through a Gibbs energy model containing reference terms, ideal mixing contributions, and excess functions describing non-ideal interactions. Parameter optimization is performed by fitting to available experimental phase-equilibrium information and reliable thermodynamic constraints.

In this framework, the unary reference Gibbs energy of an element iii is defined relative to its standard element reference (SER) state as :

$^{\circ}G_i(\mathrm{T}) = G_i(\mathrm{T}) - H_i^{SER}$

are represented by Eq.(2):

$$^{\circ}G_i(\mathrm{T}) = a + bT + cT\ln(T) + dT^2 + eT^{-1} + FT^3 + iT^4 + KT^{-9} \quad (2)$$

For substitutional solution phases, the molar Gibbs energy of a phase α\alphaα can then be expressed in the standard CALPHAD form as:

$$^{m}G^{\alpha} = X_{Fe}G_{Fe}^{\alpha} + X_{Ti}G_{Ti}^{\alpha} + RT(X_{Fe}\ln X_{Fe} + X_{Ti}\ln X_{Ti}) + (X_{Fe}X_{Ti})\sum_i [({}^{i}A + {}^{i}BT)(X_{Fe} - X_{Ti})^{i}] \quad (3)$$

Where X_{Fe} and X_{Ti} are the mole fractions of Fe and Ti, respectively, R is the universal gas constant, and T is the absolute temperature. The interaction parameters ${}^{i}A$ and ${}^{i}B$ were determined through thermodynamic optimization.

2.5.2. Reference states and unary descriptions (SGTE)

To ensure consistency with widely accepted thermodynamic conventions, the Gibbs energies of pure elements were described using the SGTE formulation, which provides standardized unary reference functions for many metallic elements [24]. In practice, Fe in the BCC_A1 structure and Ti in the HCP_A3 structure were used as SER reference states. The SGTE unary functions are commonly represented using temperature-dependent expressions over different temperature intervals, where the coefficients are adjusted accordingly.

2.5.3. Fe–Ti binary reassessment and parameter calibration

A CALPHAD reassessment of the Fe–Ti binary system was conducted to reproduce phase equilibria and key invariant reactions over a broad temperature–composition window. The optimization strategy aimed to maintain agreement with available phase-equilibrium constraints while also being compatible with the energetic stability of the main intermetallic compounds obtained by DFT. In practical terms, the DFT formation enthalpies were treated as strong energetic anchors for intermetallic stability, helping to constrain the Gibbs energy functions of compound phases and to reduce uncertainty in regions where experimental thermochemical data may be limited.

2.6. Extension to the Fe–Ti–Ag ternary system

To explore alloying-driven phase stability trends beyond the binary level, the thermodynamic description was extended to the Fe–Ti–Ag ternary system. This extension enables the study of how Ag additions influence equilibrium phase relations and stability domains. Ternary phase information provides essential context for interpreting potential stability shifts and for supporting future alloying or surface-engineering concepts. Where relevant, literature-based ternary constraints and known phase-relation observations were used as guidance to keep the ternary description physically consistent [25]. The ternary calculations were then used to generate isothermal sections and stability trends that complement the binary reassessment and support comparative interpretation of the effect of silver.

3. Results and Discussion

3.1. CALPHAD reassessment of the Fe–Ti binary system and phase-equilibrium interpretation

A reliable thermodynamic description of the Fe–Ti binary system is a fundamental requirement for predicting phase stability and microstructural evolution in Fe–Ti-containing alloys over practical processing conditions. In the present work, the CALPHAD methodology was employed to reassess phase equilibria in Fe–Ti across a broad temperature–composition range, enabling a quantitative interpretation of stability domains relevant to the appearance of ordered intermetallic phases and their sensitivity to thermal processing histories. The Fe–Ti system has been studied extensively because of its technological importance and the presence of intermediate compounds such as FeTi and Fe_2Ti , yet reported descriptions still show variations depending on the choice of models and thermodynamic assumptions. Early CALPHAD-oriented evaluations were introduced by Kaufman and Nesor [26] and further refined by subsequent assessments including Murray [27], Hari Kumar et al. [28], and Dumitrescu et al. [29].

Figure 1 shows the calculated Fe–Ti binary phase diagram obtained from the present CALPHAD reassessment, highlighting the stability domains of FeTi- and Fe_2Ti -related phases over a wide temperature–composition range and Table1 presented the reaction of Fe-Ti binary system.

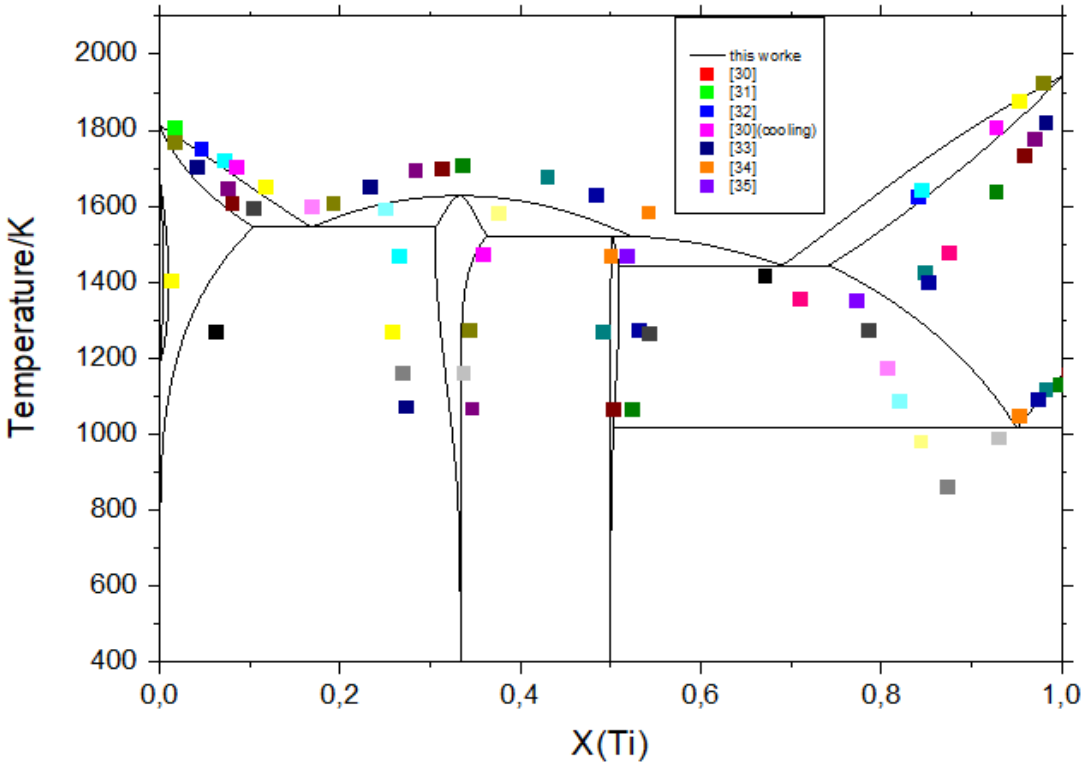

Figure 1: Calculated phase diagram of the Fe–Ti binary system obtained from the present CALPHAD assessment.

Table1 : The reaction of Fe-Ti binary system.

Réactions	T(K)	Composition (Ti at%)	Références.
L ↔Fe + Fe_2Ti	1562	-	[36]
	1599	0.25	[37]
	1566	0.275	[38]
	1559	0.260	[39]
	1560	0.30	This work
Fe_2Ti ↔L	1700	-	[36]
	1696+-6	-	[37]
	1710	0.33	[38]
	1706	0.329	[39]
	1691	0.34	This work
L + Fe_2Ti↔FeTi	1590	-	[36]
	1589+-9	-	[37]
	1578	0.5	[38]
	1592	0.492	[39]
	1608	0.395	This work
L ↔ FeTi+ BCC-Ti	1353	0.78	[36]
	1359+-7	0.77	[37]
	1355	0.676	[38]
	1352	0.77	[39]
	1350	0.70	This work
BCC-Ti ↔ FeTi+ HCP-Ti	848-873	0.86-0.87	[37]
	861	0.869	[38]
	856	0.865	[39]
	856	0.87	This work

As shown in Figure 1, the distribution of FeTi and Fe_2Ti stability fields provides a direct thermodynamic reference for interpreting phase selection during thermal processing.

A central issue in Fe–Ti thermodynamics is the accurate positioning of stability regions for FeTi and Fe_2Ti, since these intermetallic phases strongly influence microstructural reliability and mechanical response when they form during solidification or heat treatment. In practical alloy processing, phase stability is not only a theoretical matter: the occurrence of hard intermetallic phases may alter toughness and deformation behavior, particularly under thermal cycling conditions relevant to fabrication routes such as hot working, heat treatment, and welding. For this reason, the reassessment strategy in this study aimed at generating a phase-equilibrium description that remains consistent with established experimental boundaries while being sufficiently robust for coupling with energetic stability trends derived from first-principles calculations.

From a CALPHAD standpoint, the Gibbs energy functions of phases are optimized to reproduce phase boundaries, invariant reactions, and solubility limits while maintaining consistency between the descriptions of solution phases and intermediate compounds. For Fe-rich alloys, magnetic contributions can significantly affect calculated equilibria, which is why several thermodynamic formulations incorporate magnetic models to represent Fe-based phases more realistically. A representative approach addressing alloying effects in ferromagnetic metals was discussed by Hillert and Jarl [40], and additional modeling perspectives were later reported by Jönsson [41]. Incorporating these considerations is especially important when stabilizing the Fe-rich side of the diagram, where small energetic shifts can produce noticeable differences in calculated phase boundaries.

In addition to classical binary reassessments, more recent works have continued to refine Fe–Ti thermodynamic modeling by combining CALPHAD with first-principles energetics. For example, Bo et al. performed an experimental study and thermodynamic assessment of the Cu–Fe–Ti system, highlighting how CALPHAD can be constrained through multi-system consistency [42]. More directly within Fe–Ti, Santhy and Hari Kumar applied a coupled CALPHAD–VASP strategy and a multi-sublattice framework to model magnetic Laves-type behavior using first-principles input [43]. Such contributions support the underlying motivation of the present approach: DFT-derived energetic descriptors can strengthen thermodynamic optimization and reduce uncertainty, particularly when experimental thermochemical data are incomplete, scattered, or difficult to interpret.

Within this study, the reassessed Fe–Ti description was also developed with the intention of supporting extension toward Fe–Ti–Ag. The reliability of a ternary extrapolation depends strongly on the internal consistency of the underlying binaries, since additional degrees of freedom in a ternary model may amplify uncertainties if the binary thermodynamics are weakly constrained. In this regard, available experimental ternary information—such as the isothermal section work on Ag–Fe–Ti at 1123 K—provides important guidance for keeping phase relations physically meaningful when expanding beyond Fe–Ti [44].

Overall, the Fe–Ti reassessment established in this work provides a coherent equilibrium framework that supports two complementary interpretations. First, it enables a thermodynamic mapping of FeTi- and Fe_2Ti-related stability domains and clarifies composition–temperature regions where intermetallic formation is expected under equilibrium conditions. Second, it offers

a quantitative basis for linking processing windows to expected phase evolution, which is essential when interpreting microstructure development during thermal exposure in long-service engineering materials. This predictive capability becomes particularly useful when the CALPHAD optimization is supported by first-principles energetic anchors rather than relying exclusively on experimental equilibrium constraints, improving the physical credibility of the calculated stability trends.

3.2. DFT-based stability and mechanical implications of FeTi and Fe_2Ti

In addition to the CALPHAD reassessment, first-principles calculations provide a direct energetic and mechanical perspective on the stability of Fe–Ti intermetallic phases. In the Fe–Ti system, FeTi and Fe_2Ti represent two key ordered compounds whose stability and properties strongly influence phase selection and microstructure evolution. From a thermodynamic standpoint, the formation enthalpy calculated by DFT offers an atomistic measure of the driving force for compound formation, which is particularly valuable when experimental thermochemical datasets are scarce, scattered, or affected by uncertainties associated with sample preparation and phase purity.

3.2.1. Formation-enthalpy stability and comparison with literature thermochemistry

The stability of FeTi and Fe_2Ti was quantified through their calculated formation enthalpies at 0 K. This approach enables a consistent ranking of intermetallic stability and provides energetic anchors that can be used to reinforce the Gibbs-energy description in the CALPHAD assessment. Such a strategy is especially relevant for intermetallic phases because the energetic separation between competing ordered structures may be small, and equilibrium stability can be sensitive to the adopted thermodynamic parameters.

Table 1 lists the calculated structural parameters of FeTi and Fe_2Ti obtained after full geometry relaxation, which serve as the equilibrium baseline for energetic and mechanical evaluation.

Table 1: Structural parameters of the Fe-Ti system worke [45][46]

	Lattice parameter (Å)	
	A	C
Ti	2.9152193	4.6193
	2.9506	4.6825
	2.944	4.674
FeTi	2.95116145	-
	3.0175	-
	2.969	-
Fe_2Ti	4.78305	7.76722
	4.778	7.761
	4.785	7.799

These relaxed structural descriptors confirm that the subsequent property calculations are performed on equilibrium configurations.

Figure 2 compares the formation enthalpies of Fe–Ti intermetallic compounds as a function of Ti concentration, combining the present results with representative calorimetric and computational values reported in the literature.

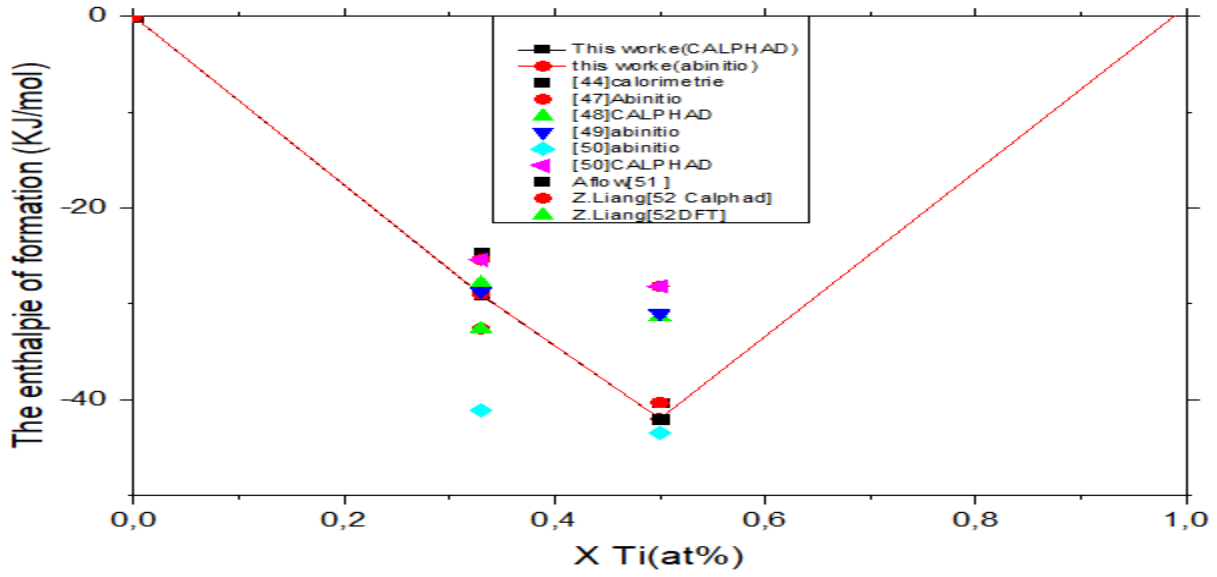

Figure 2: Formation enthalpies of Fe–Ti intermetallic compounds as a function of Ti content, comparing the present calculations with reported calorimetric and ab initio/CALPHAD literature data.

The agreement with published reference values supports the reliability of the present energetic descriptors used to anchor the thermodynamic modeling.

Experimental thermochemical investigations have previously reported formation or mixing enthalpies for FeTi and Fe_2Ti , offering an important reference point for validating computational trends. For example, Gachon et al[48]. measured enthalpy values associated with Fe_2Ti using direct reaction calorimetry at elevated temperatures, while Dinsdale and co-workers reported calorimetric formation enthalpies for FeTi, illustrating the temperature dependence and the practical challenges of extracting stable reference data for such ordered compounds [53]. The agreement between first-principles energetics and these experimental trends strengthens confidence in using DFT-derived formation enthalpies as quantitative inputs for thermodynamic reassessment.

From an engineering viewpoint, the energetic stability of these compounds also provides insight into phase-selection tendencies during processing. If a thermal exposure path enters a composition–temperature domain where FeTi or Fe_2Ti becomes highly stable, precipitation or retention of these phases may become thermodynamically favored. This is relevant for infrastructure steel concepts because the formation of hard intermetallic particles can improve strength locally but may also promote brittleness, reduce damage tolerance, and increase crack sensitivity under cyclic loading or thermal gradients.

3.2.2. Structural features and mechanical stiffness

Since civil engineering steels are often designed for long-term structural reliability rather than short-term peak strength alone, the stiffness and brittleness indicators derived from mecanical properties can be directly relevant when evaluating whether intermetallic formation is beneficial or risky in service environments.

In the present work, bulk modulus and shear modulus trends were extracted as primary measures of lattice incompressibility and resistance to shear deformation. These moduli were subsequently used to compute practical engineering descriptors such as Young’s modulus and Poisson’s ratio, which are commonly used to interpret elastic stiffness and deformation compatibility in polycrystalline materials. The use of standard polycrystalline averaging schemes provides a reasonable bridge between single-crystal elastic constants and engineering-relevant moduli. Such approaches are well established for representing realistic aggregate behavior when directional texture is not explicitly considered.

A particularly useful indicator for comparative discussion is the (B/G) ratio, which is frequently used as a qualitative measure distinguishing ductile-like and brittle-like trends in crystalline solids. While this ratio cannot replace experimental fracture or toughness testing, it provides a consistent screening metric for judging whether a given intermetallic phase may exhibit relatively brittle mechanical tendencies. In infrastructure-related steel applications, this is important because brittle intermetallic domains can introduce stress concentration points and may reduce tolerance to welding-induced residual stresses, thermal cycling, or long-term fatigue degradation.

In addition to elastic-modulus descriptors, the temperature dependence of thermodynamic functions provides complementary insight into the stability behavior of FeTi and Fe_2Ti under elevated-temperature conditions.

Figure 3 shows the temperature dependence of Gibbs free energy, entropy, and heat capacity for (a) FeTi and (b) Fe_2Ti , offering a supporting thermodynamic perspective that extends the formation-enthalpy comparison beyond 0 K.

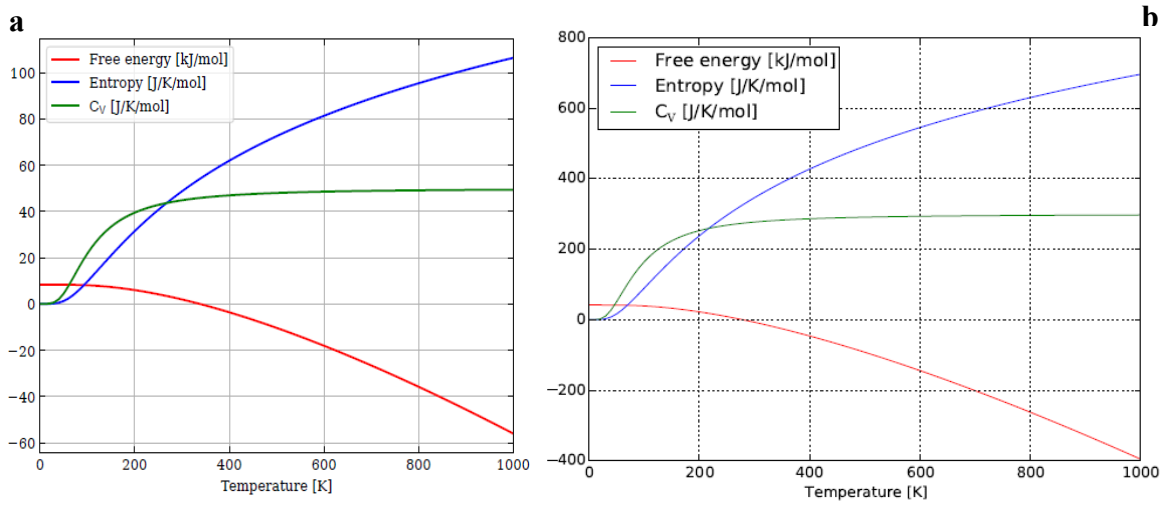

Figure 3 : Temperature dependence of Gibbs free energy, entropy, and heat capacity for (a) FeTi and (b) Fe_2Ti .

These temperature-dependent trends complement the energetic and mechanical analysis by clarifying how thermodynamic driving forces evolve with temperature for the two intermetallic phases.

3.2.3. Implications for infrastructure steel microstructures

The relevance of FeTi and Fe_2Ti is not limited to equilibrium thermodynamics, but extends to practical microstructural evolution during fabrication and service. Intermetallic compounds can form during solidification, heat treatment, or exposure to elevated temperatures, and their persistence depends on kinetic accessibility and thermodynamic driving forces. A CALPHAD–DFT workflow therefore allows phase stability predictions to be interpreted in a materials-processing context: DFT establishes stability and stiffness trends for the ordered phases, while CALPHAD maps where these phases become stable across composition and temperature.

From a civil engineering perspective, the key issue is not only whether FeTi or Fe_2Ti can exist, but how their formation would affect durability-driven performance targets such as toughness retention, deformation compatibility, and resistance to damage accumulation over long service lives. In practical terms, if FeTi or Fe_2Ti are stabilized and form as coarse or continuous regions, they can act as mechanically mismatched constituents relative to the surrounding Fe-rich matrix. Conversely, if stability and processing conditions allow these phases to remain limited in fraction or morphology, their effect may be less severe and can even be exploited in niche strengthening strategies.

3.2.4. Context from prior structural measurements

Structural characteristics and homogeneity ranges reported in the literature provide useful context for interpreting the computational results. For example, Dew-Hughes examined the effect of alloying on FeTi hydride-related behavior and reported data related to homogeneity and lattice parameters [45], while further CALPHAD-oriented studies addressing ordered Fe–Ti compounds and their stability were discussed by Keyzer et al. [46]. These references reinforce the broader conclusion that FeTi and Fe_2Ti are not only thermodynamically relevant phases, but also structurally sensitive compounds whose composition ranges and lattice behavior are important when linking thermodynamics to microstructural evolution.

Finally, when interpreting DFT formation energies in a broader computational materials-design context, it is useful to recognize that formation-enthalpy predictions are subject to systematic errors depending on functionals and dataset consistency. Large databases such as OQMD provide an established reference for assessing accuracy and trends in DFT formation energies across intermetallic systems [49]. This perspective supports the methodology adopted here, in which DFT

results are not treated as isolated outputs but are integrated into a thermodynamic modeling framework where internal consistency and phase-equilibrium compatibility are ultimately enforced.

3.3. Mechanical-property trends and engineering interpretation

While the formation-enthalpy analysis clarifies thermodynamic stability, the mechanical response of Fe–Ti intermetallic phases ultimately governs whether their presence is beneficial or detrimental for infrastructure-oriented steels. In structural applications, high stiffness may contribute to strength and dimensional stability; however, excessive brittleness or elastic incompatibility between phases can accelerate damage accumulation, promote microcracking, and reduce fracture tolerance. For this reason, the present work evaluates mechanical trends derived moduli as quantitative indicators of stiffness and deformation behavior.

3.3.1. Bulk modulus and shear modulus as stiffness descriptors

To interpret stiffness at the polycrystalline level, the bulk modulus (B) and the shear modulus (G) were extracted from the calculated elastic constants using standard polycrystalline averaging. The bulk modulus reflects resistance to volumetric compression and is relevant when discussing lattice compactness and structural rigidity. By contrast, the shear modulus is strongly linked to resistance against shape change and is often more sensitive to bonding character and shear-related deformation mechanisms. In engineering terms, (G) is a particularly important descriptor because it correlates more directly with plastic deformation resistance and, in many cases, with brittle-like mechanical trends.

Table 3 summarizes the derived polycrystalline mechanical indicators, including bulk modulus (B), shear modulus (G), Young's modulus (E), Poisson's ratio (nu), and the (B/G) ratio, which are used here to interpret stiffness and ductility-related tendencies.

Table 3 : Mechanical properties of FeTi and Fe_2Ti: this work and literature comparison [54–59].

Mechanical property	FeTi	Fe_2Ti
B(GPa)	221[this worke]	194.082[this worke]
	192[54]	-
	160.8±2[55]	-
	189[56]	-
	186[57]	-
Y(GPa)	328[this worke]	237.78[this worke]
	245[54]	-
	223[55]	-
	213[56]	-
G(GPa)	131[this worke]	91.75[this worke]
	95[54]	-
	88[55]	-
	81[56]	-
σ(GPa)	0.25[this worke]	0.30[this worke]
	0.28[54]	-
	0.26[55]	-
	0.313[56]	-
Vicher's hardness(GPa)	15.62[58]	8.64[this worke]
	16[59]	9.62[this worke]
Vicher's hardness(GPa)	1.69 (thisworke)	2.12[this worke]
B / G	2.021[54]	-
	1.818[55]	-
	2.33[56]	-
C^p (GPa)	3.2(this worke)	0.31 [this worke]
P"	0.25(this worke)	0.50 [this worke]
L'	0.59(this worke)	6780.856[this worke]
Longitudinal sound velocity(m s^{-1})	7046.288[this worke]	3580.548[this worke]
Transverse sound velocity(m s^{-1})	4051.735[this worke]	4002.799[this worke]
Average sound velocity(m s^{-1})	4499.785[this worke]	509.2[this worke]
Θ_D(K)	584.3[this worke]	

These moduli provide an engineering-oriented comparison of how FeTi- and Fe_2Ti-related constituents may influence deformation compatibility in Fe–Ti-containing steels.

3.3.2. Young's modulus and deformation compatibility

Young's modulus (E) represents the uniaxial stiffness of an isotropic elastic solid. From an infrastructure-materials perspective, (E) is crucial because it determines deformation compatibility between phases in multi-phase microstructures. If intermetallic phases exhibit substantially higher stiffness than the surrounding Fe-rich matrix, local stress concentrations can develop at phase boundaries during loading or thermal cycling. Over long service durations, this mismatch can

contribute to crack initiation and growth under fatigue or stress-corrosion conditions. For this reason, stiffness trends must be interpreted together with phase stability predictions: even a small fraction of a very stiff and brittle phase can influence the integrity of structural steels.

3.3.3. Poisson's ratio and bonding character

Poisson's ratio (\nu) provides additional insight into bonding and deformation response. Lower (\nu) values are often associated with directional bonding and limited plastic accommodation, whereas higher values tend to indicate increased shear compliance and better strain accommodation. Although Poisson's ratio alone cannot define ductility, it is valuable as a supporting descriptor—especially when it is consistent with the interpretation obtained from the (B/G) ratio.

3.3.4. Pugh's ratio (B/G): qualitative ductility–brittleness tendency

The (B/G) ratio (Pugh's criterion) is widely used as a first-order screening metric to distinguish ductile-like from brittle-like behavior in crystalline solids. A relatively high (B/G) ratio is often interpreted as a more ductile tendency, while lower values suggest higher brittleness. In the present context, this metric helps translate phase-level elastic trends into an engineering-oriented discussion relevant to service reliability.

For infrastructure steels, the implication is direct: if FeTi or Fe_2Ti phases appear within microstructures as coarse particles, continuous networks, or grain-boundary films, their brittle tendency may reduce fracture resistance and increase fatigue sensitivity. Conversely, if their formation is suppressed through careful control of composition and thermal processing (as suggested by phase-diagram constraints), the alloy may retain a more favorable balance between stiffness and damage tolerance.

3.3.5. Engineering relevance to long-service structural steels

The combined CALPHAD–DFT approach used in this work offers a practical way to link thermodynamics to mechanical performance considerations. CALPHAD predicts which phases are stable under equilibrium conditions and how stability changes with temperature, while DFT provides mechanical descriptors for the phases most likely to form. Together, these results support a durability-driven interpretation relevant to civil engineering materials: microstructures that avoid extensive intermetallic formation are expected to exhibit improved deformation compatibility and

potentially greater tolerance to long-term service conditions such as cyclic mechanical loading, welding-related residual stresses, and thermal gradients in outdoor exposure environments.

3.4. Processing and durability implications for infrastructure steel

Although the present work is primarily computational, the outcomes can be interpreted in a practical processing context that is highly relevant to infrastructure steels. In civil engineering applications, long-term performance is typically governed not only by nominal strength, but also by microstructural stability under fabrication and service conditions. In other words, a material that performs well in short-term laboratory testing may still become problematic in real structures if it develops brittle constituents, becomes sensitive to thermal cycling, or exhibits phase-instability-driven degradation over time.

3.4.1. Phase stability as a processing map

A key advantage of the CALPHAD reassessment is that it provides a thermodynamic "map" indicating which phases are expected to be stable under specific temperature–composition conditions. From an engineering viewpoint, this type of map is valuable because it transforms the phase diagram from a descriptive tool into a processing guideline. For Fe–Ti-based systems, the stability domains of FeTi and Fe_2Ti are particularly important because these ordered intermetallic phases may form during solidification, heat treatment, or extended thermal exposure. Once present, their fraction and morphology can strongly influence mechanical response.

For infrastructure steels, this matters because fabrication routes often involve complex thermal histories rather than a single controlled heat treatment. For example, steel components may experience hot rolling, controlled cooling, local reheating during welding, and in some cases stress-relief treatments. If these thermal steps intersect regions where Fe–Ti intermetallics are thermodynamically favored, precipitation may occur even if the alloy was initially designed to be predominantly Fe-rich. Therefore, understanding the stability windows of FeTi- and Fe_2Ti -related equilibria provides an essential basis for controlling microstructure and avoiding undesirable phase formation.

3.4.2. Welding and thermal cycling sensitivity

One of the most practically relevant processing challenges for civil engineering steels is welding. Welding introduces steep thermal gradients and localized exposure to elevated temperatures, often followed by relatively rapid cooling. Such thermal cycles can trigger

dissolution and re-precipitation phenomena, particularly in alloys containing strong compound-forming elements. Even when equilibrium conditions are not fully reached, CALPHAD predictions still provide a valuable baseline for identifying which phases represent the dominant thermodynamic "attractors" in different temperature regions.

Within this framework, FeTi and Fe_2Ti can be viewed as potential stability endpoints in Ti-containing steels if local composition and temperature conditions permit their formation. From a durability standpoint, this is critical because brittle intermetallic phases can act as crack-initiation sites under residual stresses and service loading. As a result, the thermodynamic description developed here supports durability-oriented processing decisions: it helps identify compositional and thermal windows where the formation of these phases is minimized, which is beneficial for maintaining fracture resistance and long-term structural reliability.

3.4.3. Microstructural reliability and deformation compatibility

Infrastructure steels are typically used in large, load-bearing components where damage tolerance, ductility, and fatigue performance are as important as strength. In such systems, microstructural reliability depends heavily on deformation compatibility between phases. If intermetallic compounds are significantly stiffer and more brittle than the surrounding matrix, elastic and plastic mismatch can increase local stress concentrations at interfaces. Over long service periods, such mismatch can accelerate microcrack formation, particularly under cyclic loading, low-temperature service, or corrosion-assisted mechanisms.

The mechanical descriptors obtained from DFT (e.g., stiffness-related moduli) therefore provide useful phase-level indicators that complement the phase-equilibrium predictions. Together, the CALPHAD and DFT results suggest that the principal engineering risk is not simply the existence of FeTi or Fe_2Ti in the phase diagram, but rather the extent to which processing routes might drive the alloy into regions where these phases become significant microstructural constituents.

3.4.4. Durability-driven interpretation for civil engineering applications

From the perspective of civil engineering materials, durability is often defined by stable performance over decades under variable environmental exposure, mechanical loading, and maintenance constraints. Within this context, the present computational approach offers two practical contributions. First, it provides a consistent thermodynamic description that can support predictive phase-equilibrium analysis as a function of temperature and composition. Second, it

supplies atomistic energetic and mechanical indicators that strengthen the interpretation of which phases are not only stable, but also potentially harmful to mechanical integrity if they develop in appreciable amounts.

While the present study does not directly model corrosion or fracture, the phase-stability framework established here is still relevant to durability because microstructural instability is frequently a precursor to degradation. Therefore, the DFT–CALPHAD workflow can be viewed as a rational screening tool: it helps identify stability-driven microstructural risks early in the design stage, and it supports durability-oriented alloy design strategies for infrastructure steel concepts where long service life and reduced maintenance are key objectives.

3.5. Optical properties (supporting/secondary section)

Although the main emphasis of the present study is placed on phase stability and mechanical reliability for durable infrastructure steels, optical-property trends were also evaluated as supporting indicators to preserve continuity with the original scope of the work. In Fe–Ti intermetallics, optical response is directly linked to the electronic structure and the distribution of available energy levels for electronic transitions. Therefore, even when optical performance is not the primary target in civil engineering applications, these calculations remain useful for confirming phase-dependent electronic differences and for highlighting functional contrasts between FeTi and Fe_2Ti. Figure 4 summarizes the calculated optical functions of FeTi and Fe_2Ti, including absorption, reflectivity, extinction coefficient, and refractive index, providing a supporting electronic-structure comparison between the two phases.

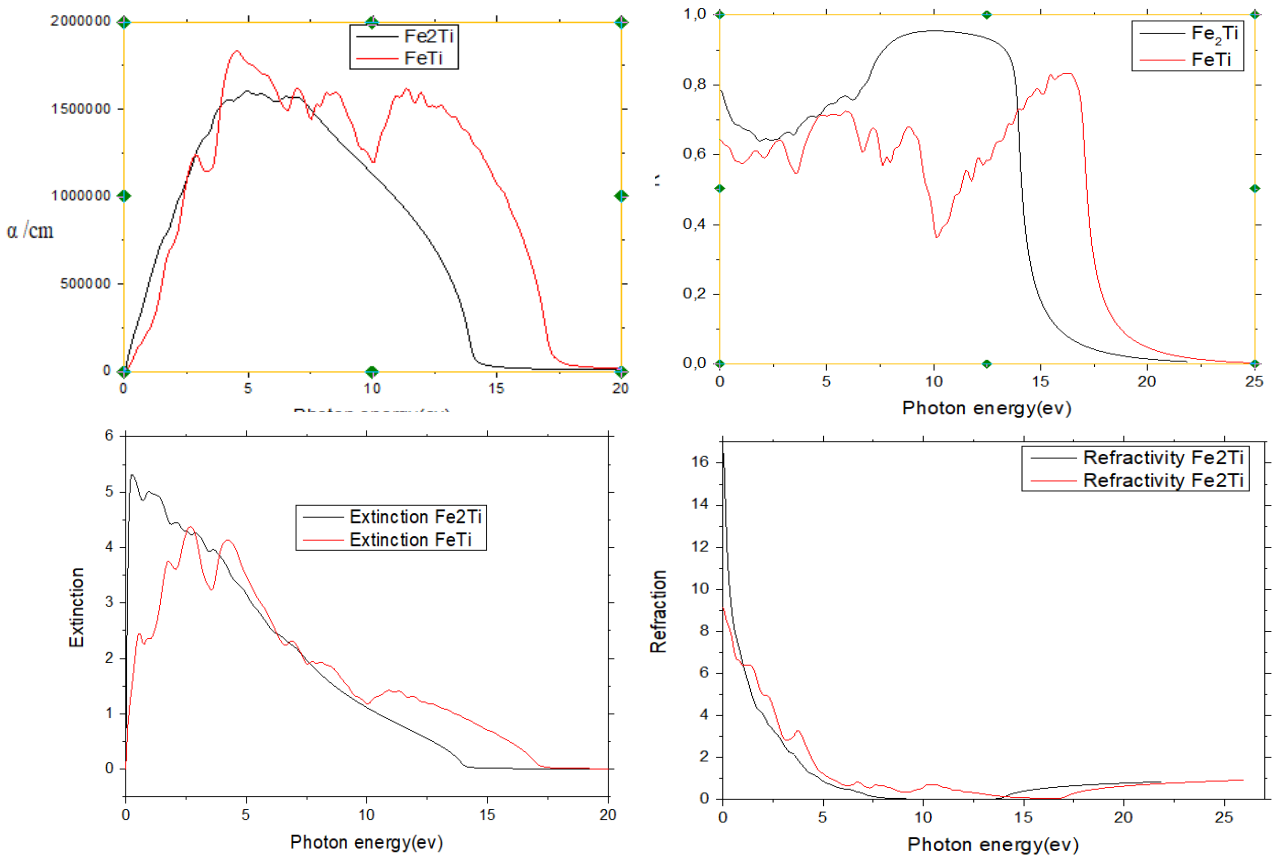

Figure 4: Variation of optical parameters as a function of photon energy: (a) absorption coefficient α, (b) reflectivity, (c) extinction coefficient, and (d) refractive index.

Although secondary to the civil-engineering focus of the study, these results reinforce that FeTi and Fe_2Ti exhibit distinct electronic responses consistent with their structural differences.

3.5.1. Absorption coefficient

The calculated absorption spectra show a clear distinction between the two intermetallic phases. FeTi displays a relatively high and broadly distributed absorption coefficient over a wide photon-energy interval, suggesting a richer set of allowed electronic transitions and a more continuous absorption capability. By contrast, Fe_2Ti exhibits lower absorption levels overall, with a more limited response that can be associated with its different symmetry and reduced electronic-transition availability compared with FeTi. This behavior is consistent with the trends reported in

Figure 4(a), where absorption in Fe_2Ti decreases more rapidly at higher photon energies, while FeTi maintains a more extended absorption window.

From a materials-interpretation standpoint, this result reinforces that FeTi behaves as a more optically active compound across a broader range of energies, whereas Fe_2Ti exhibits a more restricted absorption response. Such differences are expected for intermetallic phases with distinct crystal symmetry and electronic band characteristics, and they provide a complementary electronic-level contrast alongside the mechanical-property discussion.

3.5.2. Reflectivity behavior

The reflectivity curves further highlight phase-dependent electronic differences. As illustrated in Figure 4(b), FeTi exhibits weaker reflectivity at low energies combined with oscillatory features, indicating complex electronic transitions and energy-level structure. At higher photon energies, reflectivity remains notable before gradually declining beyond roughly 18 eV. In contrast, Fe_2Ti presents a comparatively high and nearly constant reflectivity at low energies up to about 15 eV, followed by a more abrupt drop.

These contrasting trends support the interpretation that the electronic structures of FeTi and Fe_2Ti differ significantly, which is consistent with their distinct crystallographic character. In practical terms, even though such optical signatures are not typically decisive for infrastructure steels, they remain useful as an internal consistency check showing that the two intermetallic phases cannot be treated as electronically equivalent.

3.5.3. Extinction coefficient

The extinction coefficient curves provide another perspective on attenuation and absorption intensity across photon energy. According to Figure 4(c), Fe_2Ti shows a pronounced peak at low energies followed by a gradual reduction toward near-zero values around 15 eV, indicating localized absorption behavior and relatively mild attenuation at higher energies. FeTi, however, maintains a broader extinction response with stronger oscillations up to approximately 18 eV, which suggests more intense and distributed absorption across a wider energy interval.

This difference can again be interpreted through the structural contrast between the two compounds: the cubic FeTi phase tends to support a broader range of electronic transitions, while the hexagonal Fe_2Ti phase is associated with more selective transition windows.

3.5.4. Refractive index trends

The calculated refractive-index behavior (Figure 4(d)) indicates broadly similar qualitative features for the two phases across the investigated energy range, including high values at elevated energies followed by a pronounced decrease toward low energies and stabilization near small values with minor oscillations. Although the refractive-index response does not introduce a major phase separation trend as strong as absorption or reflectivity, it still supports the overall conclusion that FeTi and Fe_2Ti display distinct optical signatures tied to their underlying electronic structures.

3.5.5. Relevance of optical trends within a civil-engineering framing

In the context of civil engineering materials, the primary value of these optical results is not direct structural design, but rather the confirmation that FeTi and Fe_2Ti differ substantially in electronic response, consistent with their mechanical and thermodynamic distinctions. Accordingly, optical-property calculations can be viewed as supportive evidence that strengthens phase-level interpretation and emphasizes that the choice of phase constitution in Fe–Ti-containing steels may also influence secondary functional properties.

3.6. Fe–Ti–Ag ternary extension: phase stability trends and interpretation

The extension from the Fe–Ti binary backbone to the Fe–Ti–Ag ternary system provides a more realistic thermodynamic view of how alloying or surface-related Ag enrichment could influence phase stability. Importantly, the purpose of this ternary investigation is not to claim that silver should be used as a conventional bulk addition in construction steels, but rather to quantify stability shifts and phase-equilibrium constraints that may become relevant in specialized durability-driven concepts, including surface alloying, functional claddings, or hybrid metallic layers.

3.6.1. Fe–Ag binary backbone and immiscibility constraint

Before interpreting ternary behavior, it is useful to recall that Fe and Ag show very limited mutual solubility. This feature places a strong constraint on ternary equilibria, because it tends to favor phase separation and limits the extent to which Ag can be incorporated into Fe-rich phases under equilibrium conditions. The calculated Fe–Ag binary phase diagram illustrates this immiscibility clearly and confirms that Fe and Ag remain essentially insoluble in one another across the composition range.

Figure 5 presents the calculated Fe–Ag binary phase diagram, confirming the strong immiscibility and limited mutual solubility between Fe and Ag over the investigated composition range.

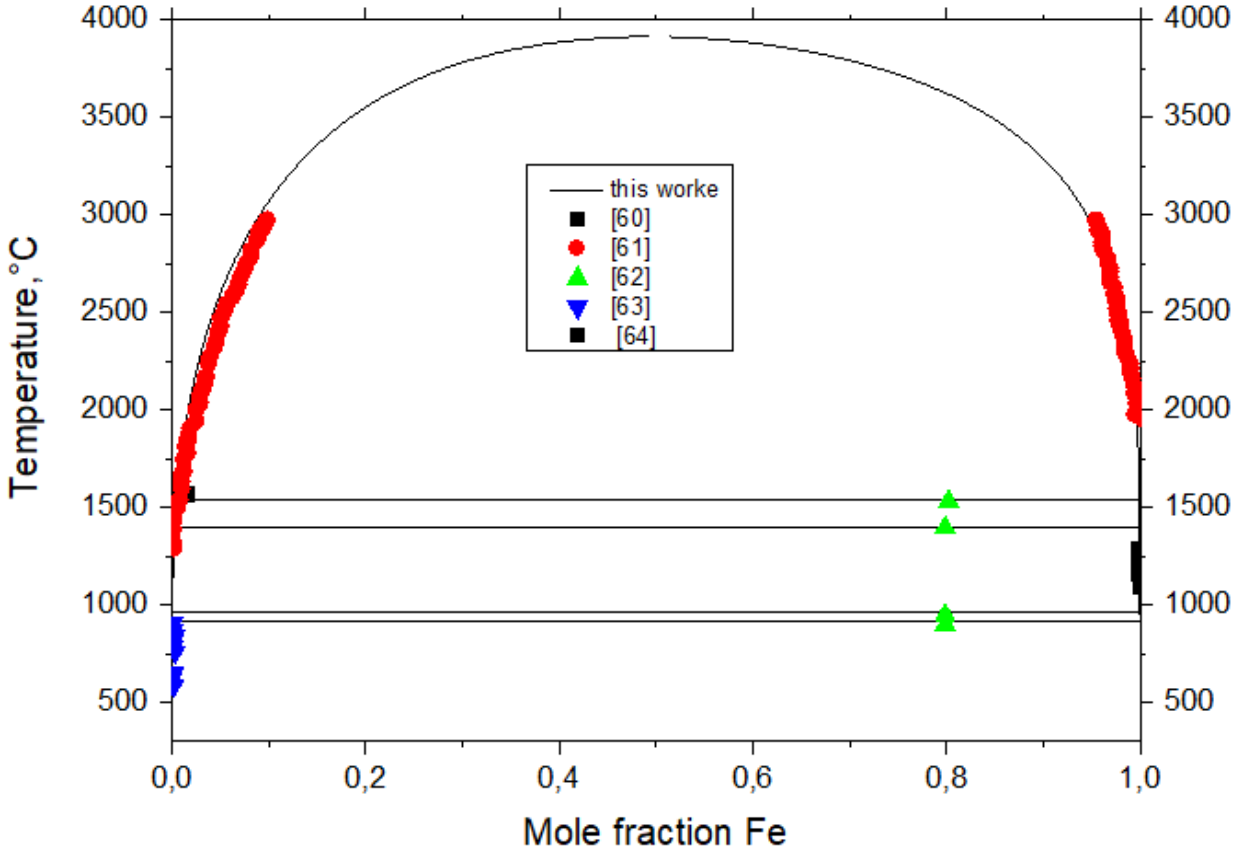

Figure 5: Phase diagram of the calculated Fe-Ag system.

Table 3 summarize Reactions of the Fe-Ag system.

Table 3: Reactions of the Fe-Ag system

Reaction	T(K)	Ref.
L 1↔ δFe+L2	1533 1499	[65] Our work
Liquid2 + (δ Fe) → (γFe)	1398 1394	[65] Our work
Liquide2 → (γ Fe) + (Ag)	961 962	[65] Our work
(γFe) → (αFe) + (Ag)	912 909	[65] Our work

This binary constraint is important because it shapes the topology of the Fe–Ti–Ag ternary equilibria and limits the extent of Ag incorporation into Fe-rich phases.

From an engineering viewpoint, this result is meaningful: it implies that any Ag-related effects in Fe–Ti–Ag are more likely to appear through phase-boundary shifts, the stabilization of Ag–Ti intermetallics, or microstructural partitioning rather than through substantial solid-solution strengthening of Fe-rich structural phases.

3.6.2. Isothermal section at 1123 K: phase fields and absence of ternary compounds

The key ternary result of this study is the calculated isothermal section of Fe–Ag–Ti at 1123 K, which indicates that no ternary compound is present under these conditions. Instead, the equilibrium constitution is governed by binary and terminal phases, with phase relations organized into multiple single-, two-, and three-phase regions.

The diagram indicates that phase equilibria are dominated by binary intermetallics (FeTi, Fe_2Ti , AgTi, and $AgTi_2$) together with the terminal solution phases.

At 1123 K, the predicted single-phase fields include Fe, Ag, βTi, FeTi, Fe_2Ti, AgTi, and $AgTi_2$. This outcome reinforces a physically consistent picture: Ag preferentially forms intermetallics with Ti (AgTi and $AgTi_2$), while Fe–Ti maintains its own ordered compounds (FeTi and Fe_2Ti), and Fe–Ag remains largely immiscible.

Beyond single-phase regions, the isotherm contains a set of two-phase domains such as Fe+Ag, Fe_2Ti+Ag, FeTi+Ag, FeTi+AgTi, FeTi+$AgTi_2$, βTi+FeTi, and βTi+$AgTi_2$. These fields reveal the thermodynamic structure of the system: in broad terms, Ag tends to coexist either with Fe-rich terminal phases or with Fe–Ti intermetallics, while Ti-rich compositions strongly favor Ag–Ti compound formation.

The calculated isotherm also contains three-phase regions, which define more restrictive equilibrium intersections that are often useful for validating the topology against experimental phase-relation observations. Examples include Fe+Ag+Fe_2Ti and Fe_2Ti+AgTi+$AgTi_2$. Such three-phase triangles are particularly informative because they represent fixed equilibrium combinations at the selected temperature and therefore offer clear constraints on phase assemblages.

3.6.3. Comparison with experimental reference data

A practical strength of the ternary extension is that it can be compared against the limited experimental information available for Ag–Fe–Ti. In the present work, the calculated isothermal section at 1123 K was contrasted with the experimental study of van Beek et al [44], which is reported as the key available reference for this system. The comparison suggests overall agreement in the main topology, while differences appear primarily in Ti-rich regions.

As shown in Figure 6, the calculated Fe–Ag–Ti isothermal section at 1123 K reproduces the main experimental phase-field topology reported by van Beek et al., supporting the reliability of the present ternary thermodynamic description.

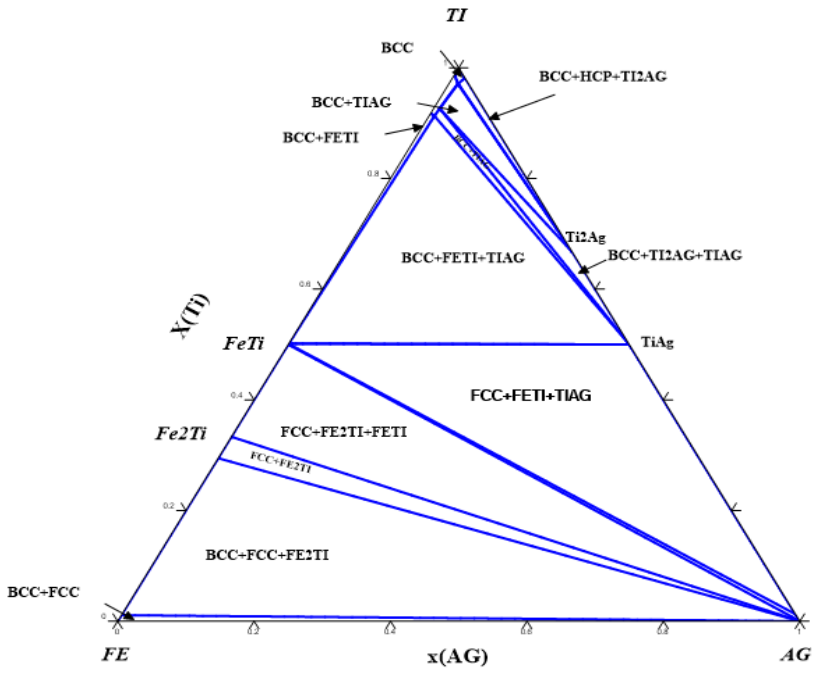

Figure 6 **:** Calculated isothermal section of the Fe–Ag–Ti ternary system at 1123 K

The remaining differences are mainly confined to Ti-rich regions, where strong Fe–Ag immiscibility and the presence of multiple Ag–Ti intermetallics can shift calculated phase boundaries with relatively small changes in assessed parameters. Such discrepancies are not unusual in ternary thermodynamic descriptions, especially when one side of the ternary has strong immiscibility (Fe–Ag) and the other side contains multiple intermetallic compounds (Ag–Ti), because small changes in assessed unary or binary parameters can shift phase boundaries noticeably in composition space.

3.6.4. Thermodynamic parameters and model consistency

The optimization of the ternary description was supported by phase-equilibrium constraints and thermodynamic information, including contributions related to the enthalpy of mixing in the liquid phase. The fitted parameter set obtained from the assessment is summarized in the thermodynamic parameter table. Table 4 reports the optimized thermodynamic parameters used to describe the Fe–Ag–Ti isothermal section at 1123 K within the CALPHAD framework.

Table 4: Parameters of the thermodynamic description of the isotherm of the Fe-Ag-Ti ternary system at 1123 K.

Phase	Parameters
Liquid	${}^{\circ}L^{FeTi}$= -71347+9.25T
	${}^{1}L^{FeTi}$=+7034-4.5T
	${}^{2}L^{FeTi}$=+12155-4.98T
	${}^{\circ}L^{FeAg}$=110114.85-9.11T
	${}^{1}L^{FeAg}$=-27699.55+6.74T
	${}^{2}L^{FeAg}$=2336.64
	${}^{\circ}L^{AgTi}$=-35625.8-2.19045T
	${}^{1}L^{AgTi}$=-1529.8+1.15291T
	${}^{2}L^{AgTi}$=12714.4-5.18624T
	${}^{3}L^{AgTi}$=1177.1
	${}^{\circ}L^{FeAgTi}$=-11475+11T
	${}^{1}L^{FeAgTi}$=-12375+11T
BCC	$^{\circ}L^{bcc}_{Fe,Ti}$=-59098+11.5T
	$1L^{bcc}_{Fe,Ti}$=+19+2T
	$2L^{bcc}_{Fe,Ti}$=+10+1.5*T
	$^{\circ}L^{bcc}_{AgFe}$ =+90000
	$^{\circ}L^{bcc}_{Ti,Ag}$=+39676-5.73T
FCC	$^{\circ}L^{FCC}_{AgTi}$=+43319.6-6.94445T
	$1L^{FCC}_{AgTi}$=+9968.8-2.83662T
	$2L^{FCC}_{AgTi}$ =3629.4

	L^{FCC}_{AgFe}=+92500
	$^{\circ}L^{FCC}_{FeTi}$=-51625+11T
	$1L^{FCC}_{Fe,Ti}$=-1950-6*T
	$2L^{FCC}_{Fe,Ti}$=+14875
HCP	$^{\circ}L^{HCP}_{FeTi}$ =-28750+11T
	$1L^{HCP}_{FeTi}$ =-1700-6T
	$2L^{HCP}_{FeTi}$ =+15000
	$^{\circ}L^{HCP}_{AgTi}$ =-2980-27T
	$^{\circ}L^{HCP}_{AgFe}$ = +199999
Fe_2Ti	$^{\circ}G^{Fe2Ti}_{Fe,Fe}$=+19000+3GHSERFE
	$^{\circ}G^{Fe2Ti}_{Ti,Ti}$ =+20000+3GHSERTI
	$^{\circ}G^{Fe2Ti}_{Fe,Ti}$ =-88199-33T+ 0.5GHSERFE+1.6GHSERTI
	$^{\circ}G^{Fe2Ti}_{Ti,Fe}$ =-31000+0.7T+GHSERFE+2GHSERTI
	$^{0}G^{Fe2Ti}_{Fe,Ti}$=+100
FeTi	$^{\circ}G^{FeTi}_{Fe,Fe}$ =-11000+0.5GTIBCC
	$^{\circ}G^{FeTi}_{Ti,Ti}$ =+27900+0.5GHSERFE+1.67GTIBCC
	$^{\circ}G^{FeTi}_{Fe,Ti}$=-88400-23T+0.5GHSERFE+0.5 GHSERTI
	$^{\circ}G^{FeTi}_{Ti,Fe}$=-42000+0.5T+GHSERFE+GHSERTI
AgTi	G^{AgTi}_{m}=-13386.21+8.7T+0.5GHSERAG+0.5GHSERTI
$AgTi_2$	G^{AgTi2}_{m}=-15096.21+9.47T+0.33GHSERAG+0.67GHSERTI

This parameter set documents the quantitative basis of the ternary description and can be refined further if additional experimental constraints become available.

From a modeling standpoint, the presence of these parameters is important for two reasons. First, they document the thermodynamic basis used to reproduce the 1123 K isothermal section in a quantitative CALPHAD framework. Second, they provide a starting point for future database

refinement if additional ternary experimental measurements become available, particularly in Ti-rich domains where uncertainty remains higher.

3.6.5. Engineering interpretation: what the ternary results mean for durable infrastructure steels

Within an infrastructure-steel framing, the ternary results should be interpreted carefully and realistically. The thermodynamic evidence from the Fe–Ag binary indicates that Ag does not readily dissolve into Fe-rich phases, limiting its role as a conventional alloying element for bulk structural steels. However, the ternary equilibrium results still provide meaningful insight: Ag has a clear thermodynamic preference to interact with Ti through compound formation, and Ag-containing equilibria may therefore influence phase selection in Ti-containing regions where local enrichment can occur.

This is particularly relevant in durability-oriented scenarios where Ag may appear locally rather than globally—for example, in surface-engineered layers, diffusion-modified coatings, or hybrid interfaces designed to provide multifunctionality. In such cases, CALPHAD ternary mapping becomes a practical tool for anticipating whether Ag additions would promote stable intermetallic formation or instead remain as separate Ag-rich constituents in equilibrium with Fe–Ti phases. Ultimately, the ternary extension strengthens the overall paper by showing that the Fe–Ti backbone can be systematically extended into higher-order systems while maintaining thermodynamic consistency .

4. Conclusions

This study presented a coupled DFT–CALPHAD computational framework to establish a consistent description of phase stability and property trends in Fe–Ti-based alloy systems, with a further extension toward the Fe–Ti–Ag ternary system. The main conclusions can be summarized as follows:

1. A thermodynamic reassessment of the Fe–Ti binary system was successfully developed using the CALPHAD approach, providing a coherent phase-equilibrium description over a broad temperature–composition range. The obtained stability fields offer a practical thermodynamic reference for interpreting intermetallic formation and processing sensitivity in Fe–Ti-containing alloys.

2. First-principles (DFT) calculations were employed to evaluate the energetic stability of the key intermetallic phases FeTi and Fe_2Ti through formation-enthalpy analysis. These energetic descriptors serve as reliable atomistic anchors that strengthen the physical consistency of the thermodynamic assessment, especially in regions where experimental thermochemical information remains limited or scattered.

3. Mechanical-property trends derived from elastic constants highlight that FeTi and Fe_2Ti exhibit distinct stiffness-related behavior. The calculated elastic moduli and ductility-related indicators provide an engineering-oriented basis to discuss phase-level deformation compatibility, supporting durability-driven interpretation of phase selection in long-service structural materials.

4. The extension to the Fe–Ti–Ag ternary system at 1123 K indicates that the ternary equilibria are governed mainly by terminal phases and binary intermetallic compounds, with no ternary compound predicted under the investigated conditions. The calculated phase relations and optimized parameters offer baseline thermodynamic guidance for exploring Ag-related stability effects in Ti-containing environments.

5. Optical-property calculations were included as supporting analysis and confirm that FeTi and Fe_2Ti display clearly different electronic/optical responses, consistent with their distinct structural and energetic characteristics. Although secondary to infrastructure-focused performance, these results provide additional confirmation of phase-dependent functional differences.

Overall, the present DFT–CALPHAD methodology provides a structured route to connect atomistic stability trends with macroscopic phase-equilibrium predictions in Fe–Ti-based systems. This combined approach can support durability-oriented alloy design decisions by clarifying stability domains and highlighting intermetallic phases that may influence processing robustness and long-term structural reliability. Future work should aim to complement the present computational assessment with targeted experimental validation, particularly regarding phase-fraction evolution under welding-like thermal cycles and property measurements under service-relevant environmental exposure.

References

[1] AMPP (formerly NACE). *IMPACT Study: The Global Cost of Corrosion.* (2016).

[2] Almaliki et al. Chloride-induced corrosion in reinforced concrete — review. *RSC Advances* (2024).

[3] Ogbemudia et al. Corrosion in concrete structures — review. *SN Applied Sciences* (Springer, 2021).

[4] Review on weathering steel bridges and atmospheric corrosion performance. *Materials* (MDPI, 2025).

[5] Morcillo et al. Atmospheric corrosion: fundamentals and long-term behavior. *Corrosion Science* (Elsevier).

[6] Wang et al. Titanium microalloying of steel — review. *International Journal of Minerals, Metallurgy and Materials* (Springer, 2022).

[7] Tedenac. CALPHAD methodology overview. In: *Thermodynamics of Crystalline Materials* (Springer).

[8] Wang et al. DFT-based database development and CALPHAD automation. *JOM* (Springer, 2013).

[9] Sundman, Jansson, Andersson. The CALPHAD approach and thermodynamic assessments. *Calphad* (Elsevier).

[10] Olson. Integrated Computational Materials Engineering (ICME) overview. *JOM* (Springer).

[11] CALPHAD applications in welding metallurgy. *Welding in the World / Journal of Welding and Joining* (review).

[12] Review on silver-based antimicrobial coatings. *International Journal of Molecular Sciences / Materials* (various).

[13] Silver nano-islands on stainless steels for antimicrobial/antiviral function. *Journal of Materials Research and Technology* (Elsevier, 2024).

[14] World Stainless. *Stainless Steel in Hygienic Applications* (Technical report).

[15] ASTM / ISO references on corrosion and durability testing (general).

[16] Studies on phase stability and precipitation in Fe-based alloys (Springer/Elsevier).

[17] W. Kohn, L.J. Sham, Self-consistent equations including exchange and correlation effects, *Phys. Rev.* 140 (1965) A1133–A1138.

[18] G. Kresse, J. Furthmüller, Efficient iterative schemes for ab initio total-energy calculations using a plane-wave basis set, *Phys. Rev. B* 54 (1996) 11169–11186.

[19] P.E. Blöchl, Projector augmented-wave method, *Phys. Rev. B* 50 (1994) 17953–17979.

[20] J.P. Perdew, K. Burke, M. Ernzerhof, Generalized gradient approximation made simple, *Phys. Rev. Lett.* 77 (1996) 3865–3868.

[21] H.J. Monkhorst, J.D. Pack, Special points for Brillouin-zone integrations, *Phys. Rev. B* 13 (1976) 5188–5192.

[22] R. Hill, The elastic behaviour of a crystalline aggregate, *Proc. Phys. Soc. A* 65 (1952) 349–354.

[23] B. Sundman, B. Jansson, J.-O. Andersson, The Thermo-Calc databank system, *CALPHAD* 9 (1985) 153–190.

[24] A.T. Dinsdale, SGTE data for pure elements, CALPHAD 15 (1991) 317–425.

[25] J.A. van Beek, A.A. Kodentsov, F.J.J. van Loo, Phase relations in the Ag–Fe–Ti system at 1123 K, J. Alloys Compd. 221 (1995) 108–113.

[26] L. Kaufman, H. Nesor, CALPHAD 2 (1978) 55–80.

[27] J.L. Murray, Bull. Alloy Phase Diagrams 2 (1981) 320–334.

[28] K.C. Hari Kumar, P. Wollants, L. Delaey, CALPHAD 18 (1994) 223–234.

[29] L.F.S. Dumitrescu, M. Hillert, N. Saunders, J. Phase Equilib. 19 (1998) 441–448.

[30] hellawell a, hume-rothery w. the constitution of alloys of iron and manganese with transition elements of the first long period [j]. phil trans r soc lond a, 1957, 249(968): 417−459.

[31] kivilahti j k, tarasova o b. the determination of the ti-rich liquidus and solidus of the ti−fe system [j]. metall trans a, 1987, 18(9): 1679−1680.

[32] murakami y, kimura h, nishimura y. an investigation on the titanium-iron-carbon system [j]. trans nat res inst met, 1959, 1(1): 7−21.

[33] mcquillan a d. the application of hydrogen equilibriumpressure measurements to the investigation of titanium alloy systems [j]. j inst metals, 1951, 79: 73−88.

[34] booker p h. ternary phase equilibria in the systems ti−fe−c, ti−co−c and ti−ni−c [d]. beaverton, or: oregon graduate center, 1979.

[35] van thyne r j, kessler h d, hansen m. the systems titanium-chromium and titanium-iron [j]. trans asm, 1952, 44: 974−989.

[36]j.l. murray, bull. alloy phase diagrams 2 (1981) 320–334.

[37] booker p h. ternary phase equilibria in the systems ti−fe−c, ti−co−c and ti−ni−c [d]. beaverton, or: oregon graduate center, 1979.

[38] k.c. hari kumar, p. wollants, l. delaey, calphad 18 (1994) 223–234.

[39] b. hong, w. jiang, l. duarte, c. leinenbach, l. li-bin, liu. hua-shan, j. zhan-peng, themodynamic re-assessment of fe-ti binary system, j.s cience direct 22(2012)2204-2211.

[40]M. Hillert, M. Jarl, Model for alloying effects in ferromagnetic metals, CALPHAD 2 (1978) 227–238.

[41] B. Jonsson, On ferromagnetic ordering and lattice diffusion—a simple model,Z. Met.kd. 83 (1992) 349–355.

[42] H. Bo , L.I.Duarte, W.J.Zhu, L.B.Liu , H.S.Liu, Z.P.Jin, C.Leinenbach, Experimental study and thermodynamic assessment of the Cu–Fe–Ti system, CALPHAD: Computer Coupling of Phase Diagrams and Thermochemistry 40 (2013) 24–33.

[43] K. Santhy , K.C. Hari Kumar, Thermodynamic modelling of magnetic laves phase in Fe–Ti system using first principle method, Intermetallics 128 (2021) 106978.

[44] j.a. van beek, a.a. kodentsov, f.j.j. van loo, phase relations in the ag-fe-ti system at 1123 k, journal of alloys and compounds 221 (1995) 108-113

[45] dew-hughes d. the addition of mn and al to the hydriding compound feti: range of homogeneity and lattice parameters [j]. metall trans a, 1980, 11(7): 1219−1225

[46] j.d. keyzer, g. cacciamani, n. dupin, p. wollants, calphad 33 (2009) 109–123

[47] gachon j c, notin m, hertz j. the enthalpy of mixing of the intermediate phases in the systems feti, coti and niti by direct reaction calorimetry [j]. thermochim acta, 1981, 48(1−2): 155−164.

[48] dinsdale a t, chart t g, putland f h. enthalpies of formation of binary phases in the fe−ni system [r]. middlesex: national physical laboratory, 1985.

[49] s. kirklin, j.e. saal, b. meredig, a. thompson, j.w. doak, m. aykol, s. rühl, c. wolverton, the open quantum materials database (oqmd): assessing the accuracy of dft formation energies, npj comput. mater. 1 (2015) 1–15.

[50] b. hong, w. jiang, l. duarte, c. leinenbach, l. li-bin, liu. hua-shan, j. zhan-peng, themodynamic re-assessment of fe-ti binary system, j.s cience direct 22(2012)2204-2211.

[51] R.H. Taylor, F. Rose, C. Toher, O. Levy, K. Yang, M. Buongiorno-Nardelli, and S. Curtarolo, A RESTful API for Exchanging Materials Data in the AFLOWLIB.org Consortium,Comput. Mater. Sci., 2014, 93, p 178-192.

[52] Thermodynamic Assessments of Ti-Al, Ti-Fe, and Ti-Al-Fe
Systems with Four-Sublattice Description of Ordered Body-
Centered Cubic Phase and Density Functional Theory Data, Zhi Liang
Ursula Kattner, Kamal Choudharry, Francesca Tavazza,Carelyn Campbell, J. Phase Equilib.

Diffus. (2024) 45:732–756.

[53] A.T. Dinsdale, A. Watson, H. Darton, K. Rutter, D. T. L. Visser, The formation enthalpies of FeTi and FeTi(_2) by calorimetric methods, Journal of Alloys and Compounds 248 (1997) 216–222.

[74] L.-F. Zhu, M. Friák, A. Udyansky, D. Ma, A. Schlieter, U. Kühn, J. Eckert ,J. Neugebauer , Ab initio based study of finite-temperature structural, elastic and thermodynamic properties of FeTi, Intermetallics 45 (2014) 11-17.
[55] Liebertz J, Stähr S, Haussühl S. Krist Tech 1980;15:1257-60.
[56] Buchenau U, Schober HR, Welter JM, Arnold G, Wagner R. Phys Rev B 1983;27: 955-62.
[57] Kellou A, Nabi Z, Tadjer A, Amrane N, Fenineche N, Aourag H. Phys Stat Sol (B) 2003;239:389e98.
[58] Chen X-Q, Intermetallics 19, 1275 (2011)

[59] Tian Y-J, Int. J. Refract. Hard Met. 33, 93–106 (2012)
[60] J. Bernardini, A. Combe-Brun, and J. Cabane, Solubility and Diffusion of Iron in Silver Monocrystals, CR Hebd. Se´ances Acad. Sci., 1969, 269, p 287-289, in French

[61] Jiaqiang Zhou, Biao Hu ,Yu Jiang,Chengliang Qiu,Yong Du, Huiqin Yin ,Thermodynamic Modeling of the Ag-X (X = B, Fe, Sm, Pu)Binary Systems , , J. Phase Equilib. Diffus, 1669-020-00813-5.

[62] L.J. Swartzendruber, The Ag-Fe (Silver-Iron) System, J. Phase Equilib., 1984, 5(6), p 560-564

[63] J. Chipman and T.P. Floridis, Activity of Aluminum in Liquid Ag-Al, Fe-Al, Fe-Al-C, and Fe-Al-C-Si Alloys, Acta Metall., 1955, 3(5), p 456-459
[64] H.A. Wriedt, W.B. Morrison, and W.E. Cole, The Solubility of Silver in c-Fe, Metall. Trans., 1973, 4(6), p 1453-1456
[65] l.j. swartzendruber, the ag-fe (silver-iron) system, j. phase equilib., 1984, 5(6), p 560-564